The Interaction of Wood Nanocellulose Dressings and the Wound Pathogen *P. aeruginosa*

Alison A. Jack[a,*], Henriette R. Nordli[b], Lydia C. Powell[a], Kate A. Powell[a], Himanshu Kishnani[a], Per Olav Johnsen[c], Brita Pukstad[b,d], David W. Thomas[a], Gary Chinga-Carrasco[c,*] Katja E. Hill[a]

[a] Advanced Therapies Group, Oral and Biomedical Sciences, Cardiff University School of Dentistry, Cardiff, CF14 4XY, UK

[b] Department of Cancer Research and Molecular Medicine, NTNU, Trondheim, Norway

[c] PFI, Høgskoleringen 6b, NO-7491 Trondheim, Norway

[d] Department of Dermatology, St. Olavs Hospital, Trondheim University Hospital, Trondheim, Norway

Corresponding author:
E-mail address: JackA1@cardiff.ac.uk (A. A. Jack)
E-mail address: gary.chinga.carrasco@pfi.no (G. Chinga-Carrasco)

Keywords: Nanocellulose, Biofilms, *Pseudomonas aeruginosa*, COMSTAT, Characterisation

ABSTRACT

Chronic wounds pose an increasingly significant worldwide economic burden (over £1 billion per annum in the UK alone). With the escalation in global obesity and diabetes, chronic wounds will increasingly be a significant cause of morbidity and mortality. Cellulose nanofibrils (CNF) are highly versatile and can be tailored with specific physical properties to produce an assortment of three-dimensional structures (hydrogels, aerogels or films), for subsequent utilization as wound dressing materials. Growth curves using CNF (diameter <20 nm) in suspension demonstrated an interesting dose-dependent inhibition of bacterial growth. In addition, analysis of biofilm formation (*Pseudomonas aeruginosa* PAO1) on nanocellulose aerogels (20 g/m^2) revealed significantly less biofilm biomass with decreasing aerogel porosity and surface roughness. Importantly, virulence factor production by *P. aeruginosa* in the presence of nanocellulose materials, quantified for the first time, was unaffected ($p>0.05$) over 24 h. These data demonstrate the potential of nanocellulose materials in the development of novel dressings that may afford significant clinical potential.

1. Introduction

Normal wound healing follows a defined process involving; coagulation, inflammation, cell proliferation, matrix repair, epithelialization and remodeling (Bjarnsholt et al., 2008). In contrast, chronic wounds are typically characterized by elevated inflammatory responses and tissue breakdown, and are slow or fail to heal, causing a considerable reduction in patient 'quality-of-life'. With a globally ageing population, the biomedical and socioeconomic burdens of chronic wounds are worsening, with annual costs in the US estimated at > $50 billion per annum and affecting 6.5 million people (2% of the population) (Jung et al., 2016). Chronic wounds are always colonized with bacteria, and the pathogen *Pseudomonas aeruginosa* is implicated in non-healing wounds (Davies et al., 2004). The ability of these opportunistic pathogens to produce a thick, mucoid wound biofilm is thought to prevent an effective response by host immune defenses, thereby impairing wound healing (Percival et al., 2012).

The most abundant naturally-occurring polymer is cellulose, which can be obtained from a variety of sources including: wood, non-woody plants, agricultural residues, algae and bacteria. In addition to bacterial cellulose (Czaja, Krystynowicz, Bielecki & Brown, 2006; Petersen & Gatenholm, 2011; Portal, Clark & Levinson, 2009), nanocellulose from wood pulp has been proposed as an appropriate material for wound dressing applications (Chinga-Carrasco & Syverud, 2014; Powell et al., 2016; Rees et al., 2015). Nanocellulose can be produced in large quantities using effective chemical pre-treatments, which facilitate deconstruction of the wood fiber wall into cellulose nanofibrils (CNF) (Chinga-Carrasco & Syverud, 2014; Saito, Nishiyama, Putaux, Vignon & Isogai, 2006; Wågberg et al., 2008). TEMPO-mediated oxidation is one of the most applied procedures for CNF production, leading to the introduction of carboxyl groups in the C6 position and small numbers of aldehyde groups (Saito & Isogai, 2004; Saito et al., 2006). TEMPO-mediated oxidation produces morphologically homogeneous CNF, having diameters less than 20 nm and lengths in the micrometer scale (Chinga-Carrasco, Yu & Diserud, 2011; Saito & Isogai, 2004). Furthermore, this material can be used to produce an assortment of three-dimensional structures e.g. strong, dense and smooth films (Fukuzumi, Saito, Iwata, Kumamoto & Isogai, 2009) and structured hydrogels and aerogels with high porosity, with capacity to absorb large quantities of moisture (Chinga-Carrasco & Syverud, 2014; Syverud, Kirsebom, Hajizadeh & Chinga-

Carrasco, 2011). We recently developed a method to produce CNF from *P. radiata* fibers, with low endotoxin levels (<50 endotoxin units/g cellulose) (Nordli, Chinga-Carrasco, Rokstad & Pukstad, 2016) and demonstrated that TEMPO CNF exhibits no toxicity towards 3T3 cells (Alexandrescu, Syverud, Gatti & Chinga-Carrasco, 2013) and primary human skin cells i.e. fibroblasts or keratinocytes (Nordli et al., 2016; Tehrani, Nordli, Pukstad, Gethin & Chinga-Carrasco, 2016). These studies suggested the potential of these materials for wound dressing applications (Nordli et al., 2016).

With the increasing economic burden chronic wounds are placing on worldwide healthcare systems, the use of non-toxic, biodegradable biopolymers from an abundant, sustainable source, such as wood CNF, for wound healing applications would be a distinct advantage in our current 'throw-away' culture. Many commercially available wound dressings possess a high capacity to absorb moisture due to their porous, three-dimensional structure. However, little attention has been paid of the effect of CNF materials (also with high moisture absorption capabilities) on biofilm formation of typical wound pathogens.

This study assessed (i) the effect of CNF hydrogels, at varying concentrations of CNF dispersion, on *Pseudomonas aeruginosa* (PAO1) growth in suspension, (ii) the effect of surface and bulk structure of CNF dressings on biofilm formation of PAO1 and, (iii) for the first time, the effects of these porous structures on pseudomonal virulence factor production.

2. Materials and Methods

2.1. CNF production

Pinus radiata pulp fibers were used as the raw material for CNF production. The carbohydrate composition of the pulp fibers has previously been reported (Chinga-Carrasco et al., 2012). TEMPO (2,2,6,6-tetramethylpiperidinyl-1-oxyl) mediated oxidation was applied as a pretreatment, using 3.8 mM NaClO/g cellulose, pH 10.5 (Saito et al., 2006). Oxidized fibers (1% w/v) were fibrillated following three passes through a Rannie 15 type 12.56X homogenizer. The degree of polymerization (DP 709), aldehyde groups (71 μM/g) and carboxyl groups (855 μM/g) have previously been quantified (Rees et al., 2015).

2.2. Sample Preparation

CNF samples were air- or freeze-dried to produce tight (films) or porous structures (aerogels), respectively. Freeze-dried samples were prepared at 0.2, 0.4 or 0.6% (w/v) CNF dispersions, frozen in petri dishes at -20ºC and freeze-dried for 48 h. Although differing CNF concentrations were used in the liquid dispersions, the actual grammage for all the resulting dried films and aerogels was 20 g/m^2. All the samples were cut into 1 or 2 cm^2 sections and sterilized by γ-irradiation (15 kGy). Commercially-available wound dressings AquaCel® and AquaCel Ag® (ConvaTec Ltd, Deeside) were used as controls.

2.3. Absorption Measurements

Fluid absorption of the test and control materials was assessed as previously described (Fulton et al., 2012). Dressing materials were cut into 1 cm^2 squares and weighed to the nearest 0.001 g. Samples were submerged in phosphate buffer saline, pH 7.4 (PBS) for 24 h, covered to prevent evaporation. Samples were then removed from the PBS and allowed to drip for 30 s and a wet weight obtained. Fluid absorption (g/g) = weight of the fluid absorbed/dressing dry weight.

2.4. Taxonomy of the samples

The varying percentages of CNF (wet weight) accounted for varying degrees of porosity in the dried materials. Once dried, there was no difference in the concentration of CNF incorporated in each of the prototype samples (20 g/m^2; Table 1**)**.

Table 1

Characteristics of the nanocellulose (CNF) materials used in this study.

Sample name	Concentration of CNF dispersion (w/v)	Sample preparation (resulting material)[a]
A0.2	0.2%	Freeze-dried (aerogel)
A0.4	0.4%	Freeze-dried (aerogel)
A0.6	0.6%	Freeze-dried (aerogel)
Film	0.2%	Air-dried (film)

[a]Grammage of all final dried materials = 20 g/m^2

2.5.Screening for the ability of CNF to support bacterial growth.

Bacterial growth and carbon utilization studies were undertaken using CNF dispersions. CNF dispersions were sterilized by γ-irradiation, and then diluted in deionized sterilized water to a final CNF concentration of 0.2, 0.4, 0.6 and 0.8%. The ability of CNF to inhibit or promote growth of *P. aeruginosa* PAO1 in planktonic culture was examined. Overnight cultures of PAO1 were diluted to OD_{600} 0.08 (colony forming units = 1 $x10^8$) in either MH broth, PBS or deionized water, and mixed 1:2 (v/v) with CNF dispersion or water in a 24 well plate. Plates were incubated at 37°C aerobically for 24 h measuring OD_{600} every hour at 600 nm (OD_{600}) in a FLUOstar Optima plate reader (BMG LABTECH).

2.6. Log_{10} reduction assay

Time kill assays adapted from Ong, Wu, Moochhala, Tan, & Lu (2008) were used to evaluate the antimicrobial efficacy of aerogel and film materials in comparison to a commercially available wound dressing (AquaCel®) control. CNF samples or AquaCel (Ag)® were added to a 6-well plate; 2×2 cm^2 per well in total. MH-broth (6 ml) and 60 µl of PAO1 overnight culture adjusted to OD_{600} 1.0 were then added to each well. Plates were incubated at 37°C, 24 h (aerobically), with shaking. To enumerate bacterial growth, 10 µl drops (3 x 10 µl per dilution) of bacterial suspension was removed from each dilution and dropped onto the surface of an MH-agar plate. The drops were air-dried before being incubated overnight at 37ºC to enumerate colony forming units (CFU/ml). Log reduction was calculated as log10 CFU/ml (initial bacteria upon challenge) minus log10 CFU/ml (surviving bacteria at time point after challenge). Bactericidal activity was defined as a ≥3 log10 CFU/ml (equivalent to ≥99.9%) reduction in bacterial numbers.

2.7. Assessment of virulence factors

Overnight cultures of *P. aeruginosa* PAO1 were adjusted to OD_{600} 1.0, and 60 µl were added to MH-broth (6 ml) in a 6-well plate and grown for 24 h ± CNF samples or AquaCel (Ag)® (2×2 cm^2). Bacterial cultures were then centrifuged (10000 *g*) for 10 min to produce a cell-free culture supernatant, used for extraction of virulence factors.

Pyocyanin pigment was extracted from the cell-free supernatant using chloroform (3:2; v/v). Pyocyanin (in the chloroform-phase) was re-extracted with 0.2 M HCl (2:1; v/v) and the absorbance read at 540 nm (Sarabhai, Sharma & Capalash, 2013).

Rhamnolipids were extracted from the cell-free supernatant using ethyl acetate (1:1, v/v), vortexed for 15 sec and centrifuged (10000 *g*, 4ºC, 5 min). The top layer was removed and the extraction repeated (x2) before allowing the ethyl acetate to evaporate overnight. Deionized water was used to dissolve the precipitate and orcinol reagent (0.19% orcinol in 53% H_2SO_4; 1:9, v/v) added. The sample was incubated at 80ºC for 30 min before reading the absorbance at 421 nm (Smyth, Perfumo, McClean, Marchant & Banat, 2010).

Protease activity was determined using 2% azocasein solution in 50 mM PBS, pH 7. The azocasein solution was incubated with the cell-free supernatant (1:1; v/v) in a total reaction volume of 400 µl, for 1 h at 37 ºC. The reaction was stopped by the addition of 500 µl 10% trichloroacetic acid, and residual azocasein removed by centrifugation (8000 *g*, 5 min). Protease absorbance was measured at 400 nm (Adonizio, Kong & Mathee, 2008).

For elastase determination, cell-free supernatant was mixed (3:1; v/v) with elastin-congo-red solution (5 mg/ml in 0.1 M Tris-HCl pH 8; 1 mM $CaCl_2$). Samples were incubated at 37 ºC, for up to 16 h, at 200 rpm, centrifuged at 3000 *g* (10 min) before absorbance was read at 490 nm (Sarabhai et al., 2013).

2.8. Microscopy characterization of CNF structures

Copper grids were immersed in a 0.01% suspension of the CNF sample and stained with uranyl acetate. Scanning Transmission Electron Microscopy (STEM) using a Hitachi S-5500 electron microscope was used to acquire images in bright field mode (x150000 magnification), using an acceleration voltage of 30 kV.

AFM imaging (tapping mode) of the film sample was performed with a Multimode AFM with Nanoscope V controller, (Digital Instruments) and images were acquired in ScanAsyst mode at room temperature. The AFM tips of spring constant value ~0.4 N/m were purchased from Bruker AFM probes. The image size was 2 µm x 2 µm, with a resolution of 1.95 nm/pixel.

The aerogels and films were freeze-dried for SEM analysis. Cross-sections of the films and aerogels were prepared by ion milling (using an IM4000 system), where the milling time was 5 hours at 2.5 kV. In addition, samples were cut from the

aerogels and films using an 8 mm punch biopsy for surface analysis. All samples were sputter-coated with gold and images acquired using a Hitachi scanning electron microscope (SEM, SU3500), in secondary electron imaging mode.

2.9. Confocal laser scanning microcopy (CLSM) and scanning electron microscopy (SEM) of biofilm growth on CNF materials

CNF samples (1 cm^2) were added to a 12-well plate to which contained MH broth (3 ml) and 60 µl of PAO1 overnight culture adjusted to OD_{600} 0.4. Plates were incubated at 37ºC in a static aerobic environment for 24 or 48 h before removing the supernatant and then washing the biofilms once with deionised water/PBS. Biofilms were stained with LIVE/DEAD® BacLight™ bacterial viability kit (Invitrogen, Paisley, UK) containing SYTO 9 dye (staining LIVE cells, green) and propidium iodide (staining DEAD cells, red) and incubated in the dark (10 min) before mounting on microscope slides with spacers, being set in Vectorshield (Vector Laboratories, UK) and having a coverslip on top, sealed with nail varnish. Biofilms were imaged with a Leica TCS SP2 confocal system (x63). Bacterial growth was quantified using COMSTAT image-analysis software (Heydorn et al., 2000).

Biofilm samples were prepared for SEM analyses by immersion in glutaraldehyde (2.5%) for 24 h, before being washed with deionised water (x4) and immersed in fresh deionised water, and then frozen (24 h) and freeze-dried for 24 h. The biofilms were then imaged on the Tescan Vega SEM at 5 kV. Additionally, the A0.6 aerogel with PAO1 biofilm growth was also ion-milled (as described above) and SEM images acquired in secondary electron imaging mode.

2.10. Statistical analysis

GraphPad Prism 3 was used to perform statistical analysis (GraphPad software Inc, La Jolla, USA) including one-way ANOVA using Tukey-Kramer post-test (growth curve data and COMSTAT data) and Dunnet's multiple comparison tests (log_{10} reduction and virulence data). $P<0.05$ was considered significant.

3. Results

3.1. Growth of P. aeruginosa PAO1 in CNF hydrogel suspensions

Irradiated CNF samples at ≥0.4% concentrations indicated dose-dependent inhibition of *P. aeruginosa* PAO1 (Fig. 1), possibly reflecting increased viscosity of

these dispersions or direct inhibition by CNF. No change in optical density was observed for CNF in either PBS or water after 24 h, indicating *P. aeruginosa* did not grow in, nor could it utilize CNF as a carbon source; growth only being observed in the presence of MH broth (Fig. S1).

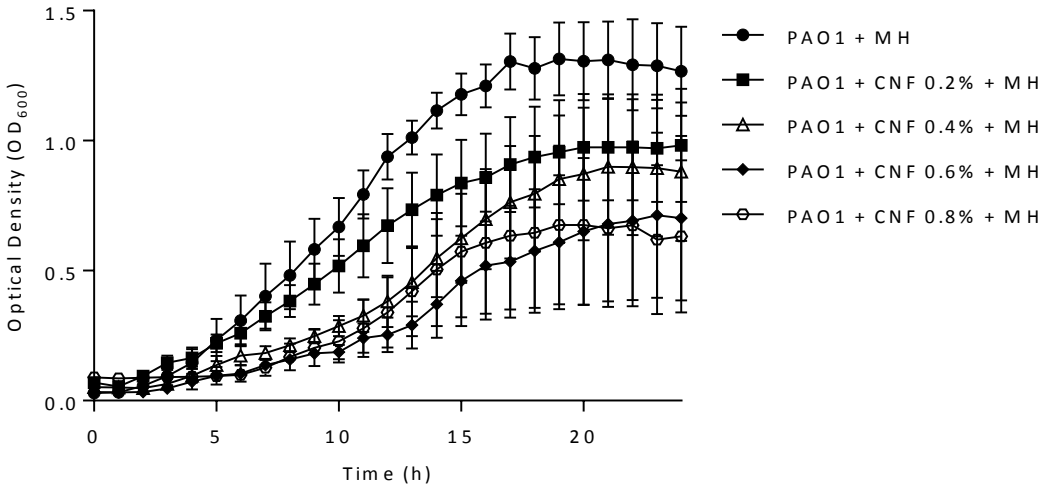

Fig. 1. Growth characteristics for *P. aeruginosa* PAO1 in CNF. *P. aeruginosa* PAO1 grown in either MH-broth/dH_2O or MH-broth/γ-irradiated CNF (adjusted to give final concentrations of CNF at 0.2, 0.4, 0.6 or 0.8%). (n=3).

3.2. Characterization of the Cellulose Materials

The CNF material was highly fibrillated and structurally homogenous (Rees et al., 2015), containing CNF with diameters in the nanoscale (<20 nm) and with a high aspect ratio, as exemplified in this study (Fig. 2).

The aerogel, A0.2 (manufactured from a 0.2% CNF dispersion) possessed the largest thickness, porosity and surface roughness, as demonstrated by SEM and fluid absorption (Fig. 3A; Table S1). The porosity and surface roughness of the other aerogels decreased with the increasing CNF concentration; A0.6 (manufactured from a 0.6% CNF dispersion) showing the lowest (Figs 3A-C). In contrast, the film was far more dense and extremely thin, with no apparent porosity (Fig. 3D). The commercial dressings AquaCel® and AquaCel Ag® displayed rough surfaces, which during the course of the experiment altered, following fluid absorption. The more porous (thicker) CNF aerogels absorbed more moisture when compared to the film; resembling absorbancy of AquaCel® and AquaCel Ag®.

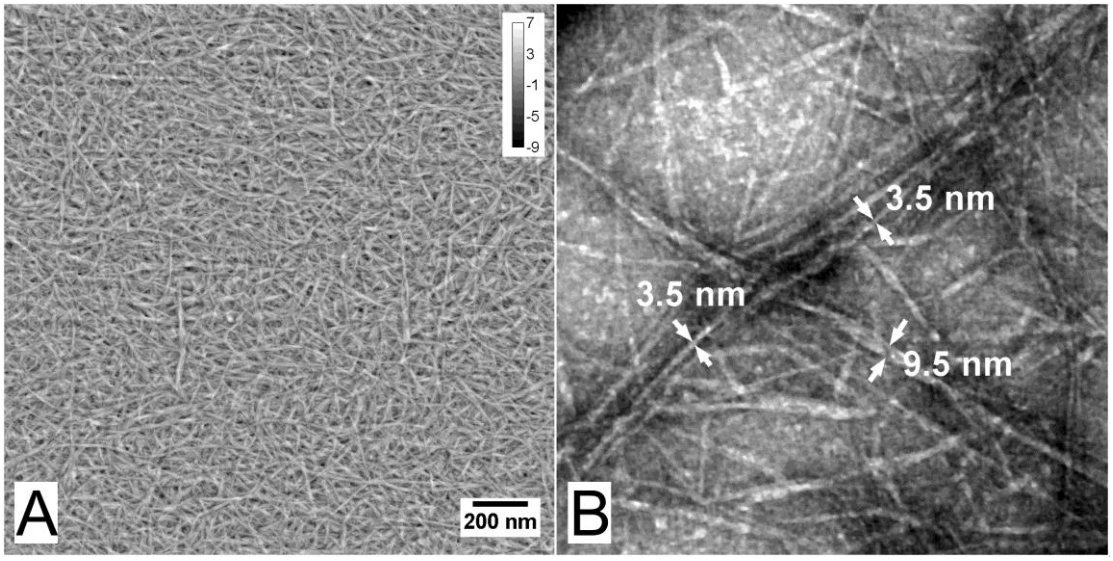

Fig. 2. Highly fibrillated nanocellulose. (A) Atomic force microscopy imaging (AFM). (B) Scanning Transmission Electron Microscopy imaging (STEM). Arrows indicate individual nanofibrils.

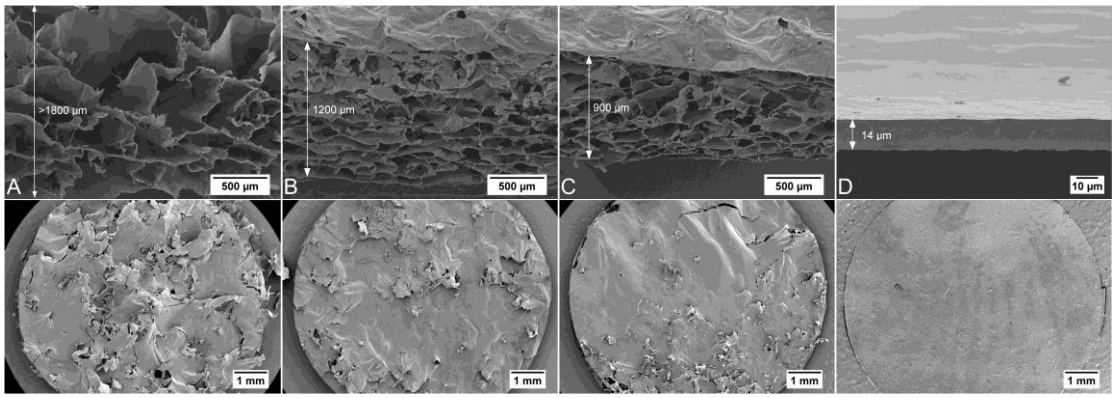

Fig. 3. Scanning electron microscopy of aerogels and films (cross-sectional and aerial views) made with CNF. (A) A0.2. (B) A0.4. (C) A0.6. (D) Film. Arrows indicate local thickness of the materials. (N.B. A0.2 was too thick to be visualized in its entirety within the maximum field of view).

3.3 Log_{10} reduction assay

The ability of CNF films and aerogels (with differing porosities) to inhibit the growth of planktonic *P. aeruginosa* PAO1 showed that none of the CNF materials, (both aerogels, 0.29-0.37±0.33-0.37 and film samples, 0.25±0.21) demonstrated significant change in Log_{10} CFU, being comparable to the negative controls AquaCel® dressing (0.24±0.16) and MH (0.38±0.37). AquaCel Ag® (the positive

control) containing ionic silver however, demonstrated significant bactericidal activity (≥3 log-fold) reduction in Log_{10} CFU compared to the control (6.62±0.94).

3.4. Virulence factor assays

The production of virulence factors (pyocyanin, rhamnolipids, total proteases and elastase) by *P. aeruginosa* PAO1 was not affected by CNF (Fig. 4). However, for elastase (measured at 1, 3 and 8 h) a significant difference to the control was detectable at ≥3 hours of incubation. A modest decreasing trend in pyocyanin production was noted based on the porosity of the aerogel materials, with A0.2 (largest pores, Fig. 3A) producing the greatest amount, whereas the A0.6 (smallest pores, Fig. 3C) and film (no pores at the assessed scale) produced the least, however this was found not to be significant.

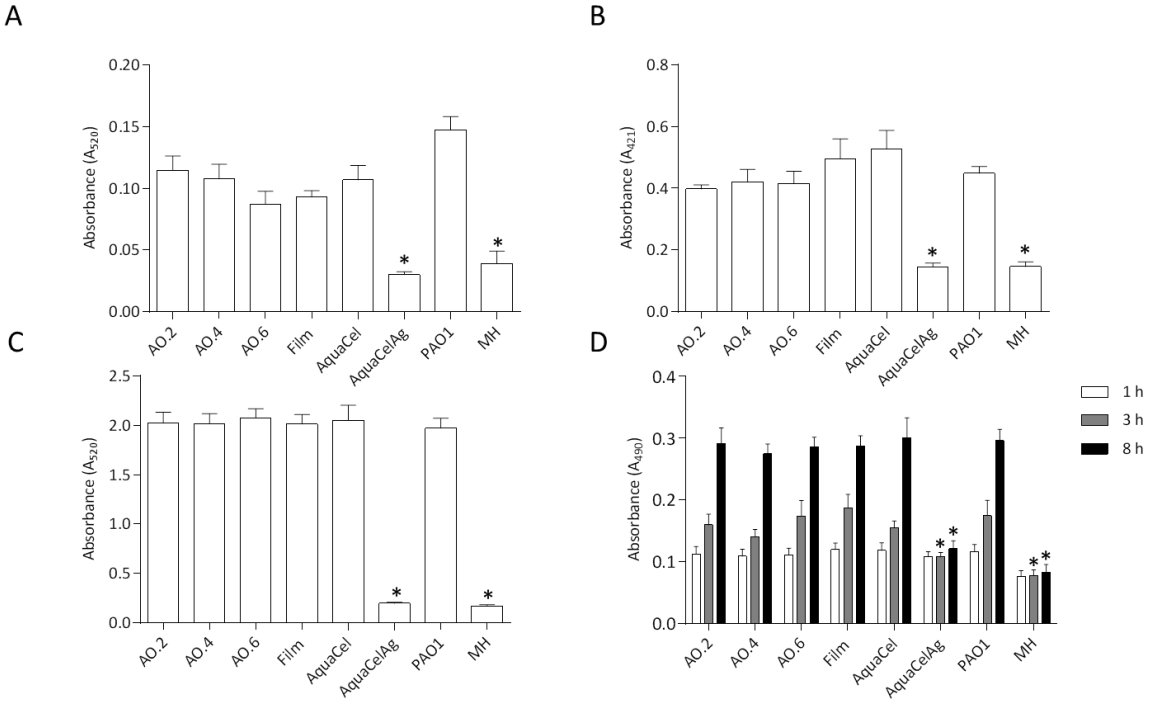

Fig. 4. The effect of the different CNF film and aerogels on virulence factor production by *Pseudomonas aeruginosa* PAO1 (A) pyocyanin. (B) rhamnolipid. (C) total protease. (D) elastase, when compared to the negative controls MH broth and AquaCel Ag®. (*significantly different as compared to the PAO1 control; n=3; $p<0.05$).

3.5. Confocal Laser Scanning Microscopy (CLSM)

P. aeruginosa PAO1 was able to form established biofilms on all the CNF and commercial (AquaCel®-based) dressing materials (Fig. 5, and Fig. S2 in the supporting information) at 24 and 48 h. LIVE/DEAD®-staining confirmed bacterial viability in the established biofilms. Little difference in bacterial viability was evident for all the dressings, (apart from AquaCel Ag® which showed sparse biofilm growth at 24 h). COMSTAT image analysis was employed to quantify biomass, surface roughness (using a roughness coefficient) and mean biofilm thickness (Fig. 5 and Fig. S2) in test samples and control Aquacel Ag®.

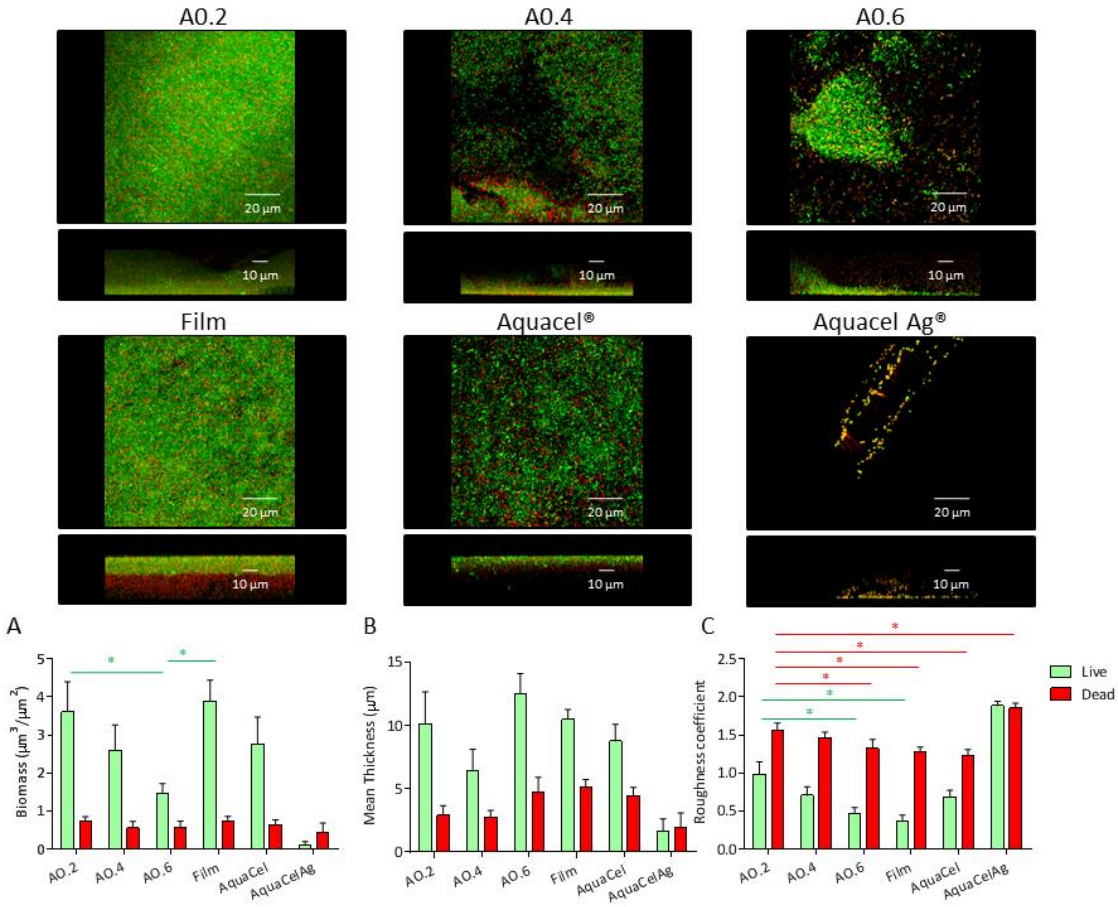

Fig. 5. CLSM images and COMSTAT analysis of LIVE/DEAD® staining of 24 h biofilms grown on CNF aerogels A0.2, A0.4 and A0.6 (0.2, 0.4 and 0.6% respectively), film and commercial dressings (Aquacel and Aquacel Ag) showing mean: (A) biomass; (B) thickness and (C) roughness coefficient (n=3, *p>0.001). All materials were significantly different to Aquacel Ag (data not shown on graphs).

COMSTAT analysis (n=7 images from n=3 replicates) revealed the viability of the biofilms and that a distinct decrease in viable cell numbers was observed between 24 and 48 h, (Fig. 5A and Fig. S2A in the supporting information**)**. In the aerogels, biomass reflected material porosity; the greatest biomass being observed in A0.2 and decreased to A0.6 (the least porous aerogel; $p<0.05$). AquaCel Ag® had very little growth at both 24 and 48 h, reflecting the CLSM.

Biofilm thickness varied between samples tested, although at 24 h these differences were less apparent (Fig. 5B**)**. As expected, mean thickness was higher on all the materials compared to AquaCel Ag® (Fig. 5B and Fig. S2B in the supporting information), with differences more apparent at 48 h.

There were significant differences in roughness coefficient between biofilms grown on the different materials, with biofilms grown on A0.2 being the roughest, while biofilms grown on A0.6 and Film were significantly smoother ($p<0.05$; 24 h); AquaCel Ag® being the roughest of all at both 24 and 48 h (Fig. 5C and Fig. S2C in the supporting information). Generally, at 48 h there were less distinguishable differences between surface roughness, probably reflecting the large proportion of non-viable cells present on all the materials at this time**.**

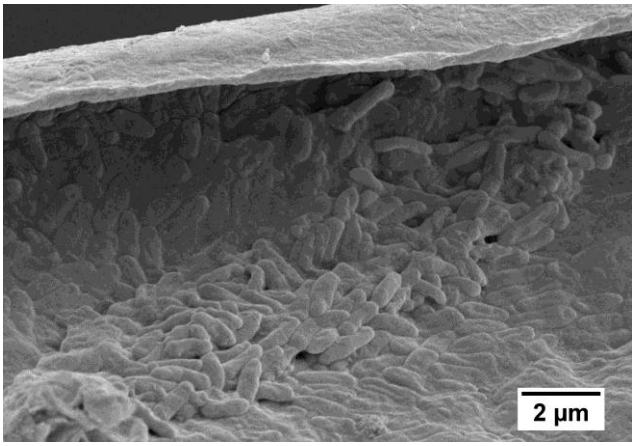

Fig. 6. SEM image of cross-section following ion milling of a *P. aeruginosa* biofilm growing on the A0.6 aerogel.

3.6.Scanning electron microscopy (SEM) of biofilm growth on CNF materials.

SEM imaging of a cross-section through a CNF aerogel following ion milling confirmed that a large part of the biofilms were formed inside the aerogel structure

(Fig. 6), probably due to the relatively large porosity of the samples. SEM imaging of the surface of the materials can be found in Figs. S3-S6 in the supporting information.

4. Discussion

It has become increasingly recognized that chronic wounds are able to sustain a substantial bacterial biofilm which (both directly and indirectly) influences clinical outcome (Hill et al., 2010). The CNF materials did not support bacterial growth of *Pseudomonas aeruginosa* PAO1, confirming that the CNF could not be used as a bacterial carbon source by the wound pathogen PAO1 (Powell et al., 2016). Materials that significantly impair microbial growth would be a distinct advantage for a wound dressing and, interestingly, a dose-dependent inhibition of bacterial growth by the CNF hydrogel was evident. This inhibition may, in part, reflect the apparent viscosity of the medium, as motile species, such as *P. aeruginosa*, move through media obtaining available nutrients (Sampedro, Parales, Krell & Hill, 2015). In keeping with this notion, the Log_{10} reduction assay revealed that CNF aerogels and films failed to inhibit microbial planktonic growth of *P. aeruginosa* PAO1 in these studies (as did the commercial wound dressing AquaCel®). The CNF materials may, therefore, exhibit distinct properties in hydrogel, aerogel or film forms.

P. aeruginosa PAO1 produces the blue pigment, pyocyanin, which is a secondary metabolite that interrupts cellular function and is also a virulence factor (Lau, Hassett, Ran & Kong, 2004) affecting mammalian cells by inhibiting cell respiration and ciliary function (Ran, Hassett & Lau, 2003; Sorensen & Klinger, 1987). Rhamnolipids are also virulence factors produced by *P. aeruginosa* which aid colonisation by acting as a surfactant, reducing surface and interfacial tension (Soberón-Chávez, Lépine & Déziel, 2005). In addition, the production of rhamnolipids in *P. aeruginosa* can enable the utilization of alternative carbon sources (such as alkanes) by pseudosolubilisation of insoluble substrates that would not normally be broken-down (Beal & Betts, 2000). *P. aeruginosa* also secretes proteases and elastase that have been implicated as virulence factors (Caballer et al., 2001), both of which are known to damage dermal matrix proteins and hinder cell migration and wound healing (Oldal & Tranfny, 2005). The lack of effect of CNF wound dressing materials on these virulence factors was characterized for the first time in the present study.

Wound dressings represent, not only a physical barrier to infection and trauma, but also incorporate antimicrobials to inhibit bacterial growth and provide an optimal (moist) environment to facilitate wound healing (i.e. cell proliferation, migration and differentiation). In close proximity to damaged skin, for considerable periods of time, they must be biocompatible. A number of natural polymers are already used as dressing materials including polysaccharides e.g. alginates and chitins, and proteins e.g. collagen (Mogoşanu & Grumezescu, 2014). Unlike bacterial nanocellulose, CNF has not traditionally been used for biomedical applications (Lin & Dufresne, 2014). Whilst a number of researchers have investigated CNF interactions in immune/inflammatory responses (Hua et al., 2015; Nordli et al., 2016), as scaffolds for cell culture (Lou et al., 2014; Ninan et al., 2013) and as spray-dried coatings (or stabilisers) for tablet production (Kolakovic et al., 2011), few have studied their interaction with the bacteria and biofilms which characterize human infection. This study clearly advances our previous studies with nanocellulose for wound dressings (Nordli et al., 2016; Powell et al., 2016), and represents novel findings in this area.

TEMPO-mediated oxidization of fibers is used to facilitate breakage of native hydrogen bonding of individual cellulose fibrils from wood cellulose fibers without causing extensive damage to the materials which would otherwise occur (Isogai, Saito & Fukuzumi, 2011). This chemical pre-treatment is followed by physical homogenization of the materials; the fibrillation process determining the characteristics of the resulting material, *i.e.* fibril size. This resultant uniform, highly-fibrillated material is suitable for a range of medical applications and may be functionalized/modified in individual biomedical applications (Lin & Dufresne, 2014). An important consideration for clinical use is sterility. The lack of structural changes in aerogels and films following γ-irradiation reflects its suitability for large-scale manufacturing/processing. The recent demonstration confirming that ultrapure CNF (lipopolysaccharide content <50 endotoxin units/gram cellulose) meets the endotoxin limits required in medical devices for wound management (Nordli et al., 2016), was also reassuring.

Three-dimensional visual assessment of the CNF CLSM images proved difficult and subjective due to the inherently rough surfaces and heterogeneous nature of the biofilms which formed. COMSTAT image analysis was therefore employed to characterize and study the biofilms formed on the materials; a technique that proved

useful. However, in terms of biomass and thickness, COMSTAT was only able to quantify changes in bacteria which remained adherent to the material surface and were visualised by CLSM. It was evident that biofilms infiltrate the dressing materials. Ion milling of biofilms growing on the materials showed that this was evident in the aerogels used in this study. Hence, the biomass and thickness data for the aerogels (being extremely porous) will have been substantially underestimated compared to those of the film (possessing no apparent pores for the biofilms to invade).

Surface roughness plays a significant role in bacteria adhesion (Hsu, Fang, Borca-Tasciuc, Worobo & Moraru, 2013; Yoda et al., 2014). This was confirmed in our study as the aerogel with the lowest surface roughness and porosity (A0.6) demonstrated the lowest biofilm growth (in terms of both thickness and biofilm height) and this was also markedly less than that observed on the commercial AquaCel® dressings. Aerogels are likely to have a clinical advantage over the film for wound applications due to their enhanced absorbency; chronic wounds often producing large amounts of exudate. This study showed that, despite having identical grammage, the aerogels (A0.2, A0.4 and A0.6) possessed distinctly different material properties (e.g. surface roughness, fluid absorption). The commercial dressings AquaCel® and AquaCel Ag® displayed an inherently rough surface, which progressively altered during the course of the experiment to become smoother with increased absorption of fluids as noted by Walker, Hobot, Newman & Bowler (2003).

Our results indicate an ability to fabricate the desired surface/pore structure of the CNF materials and their absorbance, which will be important in distinct clinical applications. For example, wound dressings should have a smooth surface (to reduce bacterial adhesion), with adequate porosity to enhance absorbency (and retain wound fluid), whilst maintaining a moist environment to promote healing. These microbiological studies show the potential use of CNF as a wound dressing material. Not only was it demonstrated that CNF dispersions did not support bacterial growth but, when the CNF dispersions were challenged with *P. aeruginosa* PAO1, bacterial growth was inhibited. Using CNF as a potential wound dressing material represents an important clinical use for this sustainable resource, with properties comparable to those of commercially-available dressings.

5. Conclusions

Our previous studies have importantly shown these materials to be non-toxic to human cells. This study confirms that CNF produced using differing manufacturing processes generates a potential wound dressing material, which allows for absorbency based on porosity to be controlled. Bacterial virulence was unaltered when grown on these materials, showing equivalency with other commercially available wound dressings already on the market. Moreover, these materials are biodegradable and may be renewably sourced; both of which are important for biosustainability. Also as the physical and chemical composition of CNF is highly malleable, the development of nanocellulose dressings offers significant clinical potential.

ASSOCIATED CONTENT

Supporting Information

Growth characteristics for *P. aeruginosa* PAO1 in CNF; Absorbancy of the CNF materials used in this study; CLSM images and COMSTAT analysis of LIVE/DEAD® staining of 48 h biofilms grown on CNF aerogels; and SEM images of 24 and 48 h *P. aeruginosa* PAO1 biofilms grown on the CNF materials.

Acknowledgements

We thank the Norwegian Micro- and Nano-Fabrication Facility for the AFM and STEM analyses (Grant no. 197411/V30). This work was funded by the Research Council of Norway through the NANO2021 program, (Grant no. 219733) – NanoHeal: Bio-compatible cellulose nanostructures for advanced wound healing applications.

References

Adonizio, A., Kong, K-F., & Mathee, K. (2008). Inhibition of quorum sensing-controlled virulence factor production in *Pseudomonas aeruginosa* by south Florida plant extracts. *Antimicrobrobial Agents & Chemotherapy*, *52*(1), 198–203.

Alexandresku, L., Syverud, K., Gatti, A. & Chinga-Carrasco, G. (2013). Cytotoxicity tests of cellulose nanofibril-based structures. *Cellulose*, *20*(4), 1765-1775.

Beal, R., & Betts, W. B. (2000). Role of rhamnolipid biosurfactants in the uptake and mineralization of hexadecane in *Pseudomonas aeruginosa*. *Journal of Applied*

Microbiology, 89(1), 158-168.

Bjarnsholt, T., Kirketerp-Møller, K., Jensen, P.Ø., Madsen, KG., Phipps, R., Krogfelt, K., Høiby, N., & Givskov, M. (2008). Why chronic wounds will not heal: a novel hypothesis. *Wound Repair & Regeneration, 16*(1), 2-10.

Caballero, A. R., Moreau, J. M., Engel, L. S., Marquart, M. E., Hill, J. M., & O'Callaghan, R. (2001). *Pseudomonas aeruginosa* protease IV enzyme assays and comparison to other *Pseudomonas* proteases. *Analytical Biochemistry, 290*(2), 330–337.

Chinga-Carrasco, G., Yu, Y., & Diserud, O. (2011). Quantitative electron microscopy of cellulose nanofibril structures from *Eucalyptus* and *Pinus radiata* kraft pulp fibres. *Microscopy & Microanalysis, 17*(4), 563-571.

Chinga-Carrasco, G., & Syverud, K. (2014). Pretreatment-dependent surface chemistry of wood nanocellulose for pH-sensitive hydrogels. *Journal of Biomaterials Applications, 29*(3), 423-432.

Chinga-Carrasco, G., Kuznetsova, N., Garaeva, M., Leirset, I., Galiullina, G., Kostochko, A., & Syverud, K. (2012). Bleached and unbleached MFC nanobarriers - properties and hydrophobization with hexamethyldisilazane. *Journal of Nanoparticle Research, 14*(12), 1-10.

Czaja, W., Krystynowicz, A., Bielecki, S., & Brown Jr, R. M. (2006). Microbial cellulose—the natural power to heal wounds. *Biomaterials, 27*(2), 145-151.

Davies, CE., Hill, KE., Wilson, MJ., Stephens, P., Hill, CM., Harding, KG., & Thomas, DW. (2004). Use of 16S ribosomal DNA PCR and denaturing gradient gel electrophoresis for analysis of the microfloras of healing and nonhealing chronic venous leg ulcers. *Journal of Clinical Microbiology, 42*(8), 3549-3557

Fukuzumi, H., Saito, T., Iwata, T., Kumamoto, Y., & Isogai, A. (2009). Transparent and high gas barrier films of cellulose nanofibers prepared by TEMPO-mediated oxidation. *Biomacromolecules 10*(1), 162–165.

Fulton, J. A., Blasiole, K. N., Cottingham, T., Tornero, M., Graves, M., Smith, L. G., Mirza, S., & Mostow, E. N. (2012). Wound dressing absorption: A comparative study. *Advances in Skin Wound Care, 25*(7), 315-320.

Heydorn, A., Nielsen, A. T., Hentzer, M., Sternberg, C., Givskov, M., Ersbøll, B. K., & Molin, S. (2000). Quantification of biofilm structures by the novel computer program COMSTAT. *Microbiology, 146*(10), 2395–2407.

514 Hill, K.E., Malic, S., McKee, R., Rennison, T., Harding, K.G., Williams, D.W., &
515 Thomas, D.W. (2010). An *in vitro* model of chronic wound biofilms to test wound
516 dressings and assess antimicrobial susceptibilities. *Journal of Antimicrobial*
517 *Chemotherapy 65*(6), 1195-1206.
518 Hsu, L. C., Fang, J., Borca-Tasciuc, D. A., Worobo, R. W., & Moraru, C. I. (2013).
519 Effect of micro- and nanoscale topography on the adhesion of bacterial cells to
520 solid surfaces. *Applied & Environmental Microbiology* 2013, *79*(8), 2703–2712.
521 Hua, K., Ålander, E., Lindström, T., Mihranyan, A., Strømme, M., & Ferraz, N.
522 (2015). Surface chemistry of nanocellulose fibers directs monocyte/macrophage
523 response. *Biomacromolecules*, *16*(9), 2787−2795.
524 Isogai, A., Saito, T., & Fukuzumi, H. (2011). TEMPO-oxidized cellulose nanofibers.
525 *Nanoscale, 3*(1), 71-85.
526 Jung, K., Covington, S., Sen, S. K., Januszyk, M., Kirsner, R. S., Gurtner, G. C., &
527 Shah, N. H. (2016). Rapid identification of slow healing wounds. *Wound Repair &*
528 *Regeneration, 24*(1),181-188.
529 Kolakovic, R,, Peltonen, L., Laaksonen, T., Putkisto, K., Laukkanen, A., & Hirvonen
530 (2011). Spray-dried cellulose nanofibers as novel tablet excipient. J. *AAPS*
531 *PharmSciTech.*, *12*(4), 1366–1312.
532 Lau, G. W., Hassett, D. J., Ran, H., & Kong, F. (2004). The role of pyocyanin in
533 *Pseudomonas aeruginosa* infection. *Trends in Molecular Medicine, 10*(12), 599-
534 606.
535 Lin, N. & Dufresne, A. (2014). Nanocellulose in biomedicine: Current status and
536 future prospect. *European Polymer Journal 59*, 302–325.
537 Lou, Y. R., Kanninen, L., Kuisma, T., Niklander, J., Noon, L. A., Burks, D., Urtti, A.,
538 & Yliperttula, M. (2014). The use of nanofibrillar cellulose hydrogel as a flexible
539 three-dimensional model to culture human pluripotent stem cells. *Stem Cells &*
540 *Development*, *23*(4), 380−392.
541 Mogoşanu, G. D., & Grumezescu, A. M. (2014). Natural and synthetic polymers for
542 wounds and burns dressing. *International Journal of Pharmaceutics*, *463*(2), 127-
543 136.
544 Ninan, N., Muthiah, M., Park, I-K., Elain, A., Thomas, S., & Grohens, Y. (2013).
545 Pectin/carboxymethyl cellulose/microfibrillated cellulose composite scaffolds for
546 tissue engineering. *Carbohydrate Polymers*, *98*, 877–98.

Nordli, H. R., Chinga-Carrasco, G., Rokstad, A. M., & Pukstad, B. (2016). Producing ultrapure wood cellulose nanofibrils and evaluating the cytotoxicity using human skin cells. *Carbohydrate Polymers,* DOI:10.1016/j.carbpol.2016.04.094.

Oldak, E., & Trafny, E.A. (2005). Secretion of proteases by *Pseudomonas aeruginosa* biofilms exposed to ciprofloxacin. *Antimicrobial Agents & Chemotherapy*, *49*(8), 3281-3288.

Ong, S-Y., Wu, J., Moochhala, S. M., Tan, M. H., & Lu, J. (2008). Development of a chitosan-based wound dressing with improved hemostatic and antimicrobial properties. *Biomaterials*, *29*(32), 4323–4332.

Percival, S. L., Hill, K. E., Williams, D. W., Hooper, S. J., Thomas, D. W., & Costerton, J. W. (2012). A review of the scientific evidence for biofilms in wounds. *Wound Repair Regeneration, 20*(5), 647–657.

Petersen, N., & Gatenholm, P. (2011). Bacterial cellulose-based materials and medical devices: current state and perspectives. *Applied Microbiology & Biotechnology*, *91*(5), 1277-1286.

Portal, O., Clark, W. A., & Levinson, D. J. (2009). Microbial cellulose wound dressing in the treatment of nonhealing lower extremity ulcers. *Wounds*, *21*(1), 1-3.

Powell, L. C., Khan, S., Chinga-Carrasco, G., Wright, C. J., Hill, K. E., & Thomas, D. W. (2016). An investigation of *Pseudomonas aeruginosa* biofilm growth on novel nanocellulose fibre dressings. *Carbohydrate Polymers*, *137*, 191-197.

Ran, H., Hassett, D. J., & Lau, G. W. (2003). Human targets of *Pseudomonas aeruginosa* pyocyanin. *Proceedings of the National Academy of Sciences, USA, 100*(24), 14315–14320.

Rees, A., Powell, LC., Chinga-Carrasco, G., Gethin, DT., Syverud, K., Hill, KE., & Thomas, DW. (2015). 3D Bioprinting of carboxymethylated-periodate oxidized nanocellulose constructs for wound dressing applications. *BioMed Research International*, *2015*, 925757.

Saito, T., & Isogai, A. (2004). TEMPO-mediated oxidation of native cellulose. the effect of oxidation conditions on chemical and crystal structures of the water-insoluble fractions. *Biomacromolecules, 5*(5), 1983–1989.

Saito, T., Nishiyama, Y., Putaux, JL., Vignon, M., & Isogai, A. (2006). Homogeneous suspensions of individualized microfibrils from TEMPO-catalyzed oxidation of native cellulose. *Biomacromolecules, 7*(6), 1687-1691.

Sampedro, I., Parales, R. E., Krell, T., & Hill, J. E. (2015). *Pseudomonas* chemotaxis.

FEMS Microbiology Reviews, *39*, 17-46.

Sarabhai, S., Sharma, P., & Capalash, N. (2013). Ellagic acid derivatives from Terminalia chebula Retz. downregulate the expression of quorum sensing genes to attenuate *Pseudomonas aeruginosa* PAO1 virulence. *PLoS One*, *8*(1), e53441

Smyth, T. J. P., Perfumo, A., McClean, S., Marchant, R., & Banat, I. M. (2010). In: K. N. Timmis (Ed.), *Handbook of Hydrocarbon and Lipid Microbiology* (pp. 3689-3704) Heidelberg: Springer-Verlag.

Soberón-Chávez, G., Lépine, F., & Déziel, E. (2005). Production of rhamnolipids by *Pseudomonas aeruginosa*. *Appl*. *Microbiol*. *Biotechnol*., *68*(6), 718–725.

Sorensen, R. U., & Klinger, J. D. (1987). Biological effects of *Pseudomonas aeruginosa* phenazine pigments. *Antibiotic Chemotherapy*, *39*, 113–124.

Syverud, K., Kirsebom, H., Hajizadeh, S., & Chinga-Carrasco, G. (2011). Cross-linking cellulose nanofibrils for potential elastic cryo-structured gels. *Nanoscale Research Letters 6*, 626.

Tehrani, Z., Nordli, H. R., Pukstad, B., Gethin, D.T., & Chinga-Carrasco, G. (2016). Translucent and ductile nanocellulose-PEG bionanocomposites – a novel substrate with potential to be functionalized by printing for wound dressing applications. *Industrial Crops & Products,* DOI:10.1016/j.indcrop.2016.02.024.

Walker, M., Hobot, JA., Newman, GR., & Bowler, PG. (2003). Scanning electron microscopic examination of bacterial immobilisation in a carboxymethyl cellulose (AQUACEL) and alginate dressings. *Biomaterials*, *24*(5), 883-890.

Wågberg, L., Decher, G., Norgren, M., Lindström, T., Ankerfors, M., & Axnäs, K. (2008). The build-up of polyelectrolyte multilayers of microfibrillated cellulose and cationic polyelectrolytes. *Langmuir*, *24*(3), 784–795.

Yoda, I., Koseki, H., Tomita, M., Shida, T., Horiuchi, H., Sakoda, H., & Osaki, M. (2014). Effect of surface roughness of biomaterials on *Staphylococcus epidermidis* adhesion. *BMC Microbiology*, *14*, 234.